

# An IBEM-FEM model of the Rayleigh wave-scattering function of long walls

David A. S. Carneiro, Josué Labaki, Pêrsio L. A. Barros

*School of Mechanical Engineering, University of Campinas  
200 Mendeleyev St, Cidade Universitária Zeferino Vaz, 13083-860, Campinas SP, Brazil  
13083-860, Campinas SP, Brazil  
d265008@dac.unicamp.br, labaki@unicamp.br, persio@unicamp.br*

**Abstract.** This work presents a numerical method to investigate the ground vibration screening capability of long walls and how their presence affects the wave propagation in the soil. Incident Rayleigh waves impinging on the wall are considered as seismic excitation. The soil is modeled as a two-dimensional, homogeneous, transversely isotropic, viscoelastic half-space modeled through an indirect formulation of the Boundary Element Method (IBEM), discretized by constant boundary elements. The method consists of a superposition of Green's functions for uniformly distributed surface loads. The wall is discretized by linear-elastic, four-noded, isoparametric, quadrilateral finite elements. This coupling results in an IBEM-FEM model in which traction and displacement fields within the half-space containing the wall subjected to Rayleigh waves are related through sets of contact tractions applied to the boundary elements. Post-processing from these tractions yields quantities such as the displacement and strain fields within the half-space, which are used to study how the presence of the wall affects the ground vibration generated by Rayleigh waves.

**Keywords:** Heavy Surface Structures, Rayleigh Waves, Ground Vibration Attenuation, Boundary Element Method

## 1 Introduction

In dynamic soil-structure interaction models, the indirect version of the boundary element method (IBEM) is occasionally used to model the soil instead of the classical boundary element method. In this approach, displacement and traction fields are connected through a set of contact tractions. A post-processing procedure from these contact tractions yields quantities such as the displacement fields and quantities deriving from this anywhere in the half-space. This enables an accurate description of wave propagation disturbance in the soil due to the presence of structures placed along the wave propagation path. This article investigates the ground vibration attenuation performance of heavy surface walls and how it affects the energy propagation from incident Rayleigh waves (Fig. 1a). Green's functions necessary for modeling the soil part are obtained from a classical solution in terms of Fourier transforms [1]. The method consists of a superposition of Green's functions for uniformly distributed surface loads. Kinematic compatibility and equilibrium conditions are imposed at the wall-soil interface, where the difference between finite and boundary element nodes locations are taken into account. The two-dimensional problem considers a plane strain case, which means that the wall is an infinitely long structure in the off-plane direction.

Krylov [2] observed that surface masses placed on the wave propagation path significantly affect ground vibration. These effects were related to the resonant behavior of the structure, which is capable of generating a surface wave scattering effect yielding reflected, transmitted, and scattered portions. Dijkmans et al. [3] presented a computationally efficient 2.5D coupled finite and boundary element model of heavy surface walls designed to study the mitigation of ground-borne vibrations. Their work detailed how the installation of a line mass, rigid cross-section, flexible, and stiffer walls at the soil surface under the effect of several types of dynamic sources attenuates ground vibration.

In this work, the wall-soil coupling results in an IBEM-FEM model in which traction and displacement fields within the half-space are related through sets of contact uniformly distributed tractions applied to the boundary

elements. Displacement and strain fields are evaluated throughout the half-space, representing the elastic wave propagation after the installation of the wall. The results show that the presence of the wall scatters surface waves into pressure and shear body waves. This deflection of energy from the surface to the bulk of the soil makes the wall an attractive strategy to protect surface structures against ground vibration.

## 2 Problem statement

Consider a two-dimensional, transversely isotropic, homogeneous, viscoelastic half-space, the plane of isotropy of which is parallel to its free surface. The medium is described by four independent elastic constants  $c_{11}$ ,  $c_{13}$ ,  $c_{33}$ , and  $c_{44}$ , mass density  $\rho_s$ , and damping factor  $\eta_s$ . An infinitely long wall of width  $L$  and height  $h$  is in bonded contact to the surface of the half-space, the center of which is aligned with the origin of the coordinate system. Ground vibrations are generated by Rayleigh (R) waves (Fig. 1a). The two-dimensional model considers a plane strain case, which means the wall and the soil are invariant with respect to the  $y$ -direction.

The coupling illustrated in Fig 1b considers a wall modeled by linear-elastic, four-noded, plane strain, isoparametric quadrilateral finite elements placed on the surface of the half-space, which is modeled by an indirect formulation of the boundary element method. Coupling between the wall and half-space systems is obtained through kinetic compatibility and equilibrium conditions imposed at the interface, which is discretized such that there is one finite element (FE) of the structure corresponding to each boundary element (BE) of soil. The latter considers displacements and tractions to be uniformly distributed along its width. This IBEM-FEM coupling model carefully considers the difference between FE and BE nodes locations.

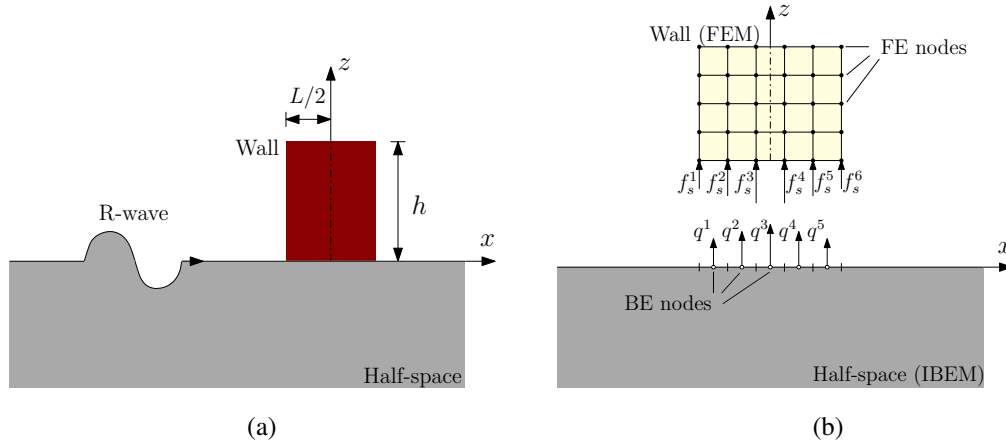


Figure 1. (a) Surface wall coupled to the homogeneous half-space under the effect of Rayleigh wave and (b) nodal contact forces and contact tractions at the interface.

## 3 IBEM-FEM formulation for seismic excitation

In this coupling formulation, the influence of the presence of the soil is incorporated in the response of the structure through a set of equivalent nodal contact forces  $\mathbf{f}_s$ , such that the dynamic equation of motion at the interface is given by:

$$\bar{\mathbf{K}}' \mathbf{u}' = \mathbf{f}' - \mathbf{f}_s, \quad (1)$$

in which the apostrophe marks quantities related to the nodes at the interface,

$$\mathbf{u}' = \{u_x^1 \quad u_z^1 \quad u_x^2 \quad u_z^2 \quad \dots \quad u_x^{n_n} \quad u_z^{n_n}\}_{2n_n \times 1}^T, \quad \mathbf{f}' = \{f_x^1 \quad f_z^1 \quad f_x^2 \quad f_z^2 \quad \dots \quad f_x^{n_n} \quad f_z^{n_n}\}_{2n_n \times 1}^T, \quad (2)$$

are respectively the nodal displacement and force vectors,  $\bar{\mathbf{K}}'$  is the dynamic stiffness matrix of the wall, and  $\mathbf{f}_s = \{f_{sx}^1 \quad f_{sz}^1 \quad f_{sx}^2 \quad f_{sz}^2 \quad \dots \quad f_{sx}^{n_n} \quad f_{sz}^{n_n}\}_{2n_n \times 1}^T$ , where  $n_n$  is the number of FE nodes at the interface. The number of nodes in the BE discretization ( $n_s$ ) is incompatible with those of the FE discretization. Describing

the distribution of unknown constant contact tractions  $\mathbf{q} = \{q_x^1 \ q_z^1 \ q_x^2 \ q_z^2 \ \dots \ q_x^{n_s} \ q_z^{n_s}\}_{2n_s \times 1}^T$  in terms of nodal equivalents  $\mathbf{f}_s$  must account for this difference, as shown in Fig. 1b.

The relation between the nodal contact forces and the contact tractions is obtained through:

$$\mathbf{f}_s = \mathbf{A}\mathbf{q}, \quad (3)$$

in which

$$\mathbf{A} = \frac{1}{2} \begin{bmatrix} l_e^1 & 0 & & & & & & & \\ & 0 & l_e^1 & & & & & & \\ l_e^1 & 0 & l_e^2 & 0 & & & & & \\ & 0 & l_e^1 & 0 & l_e^2 & & & & \\ & & & l_e^2 & 0 & & & & \\ & & & & 0 & l_e^2 & & & \\ & & & & & & \ddots & & \\ & & & & & & & l_e^N & 0 \\ & & & & & & & 0 & l_e^N \\ & & & & & & & l_e^N & 0 \\ & & & & & & & 0 & l_e^N \end{bmatrix}_{2n_n \times 2n_s} \quad (4)$$

is the force transformation matrix,  $l_e$  is the length of the FE element  $i = (i, N)$ , and  $N = n_n - 1$  is the number of FE at the interface. Substituting eq. (3) into eq. (1) gives the equilibrium equation for the nodes of the structure at the interface, which is given by:

$$\bar{\mathbf{K}}'\mathbf{u}' + \mathbf{A}\mathbf{q} = \mathbf{f}'. \quad (5)$$

In order to establish kinematic compatibility between the soil and the structure, the displacement of each BE can be written, in terms of nodal equivalents displacements, as:

$$\mathbf{u}_s = \mathbf{D}\mathbf{u}', \quad (6)$$

in which  $\mathbf{u}_s = \{u_{sx}^1 \ u_{sz}^1 \ u_{sx}^2 \ u_{sz}^2 \ \dots \ u_{sx}^{n_s} \ u_{sz}^{n_s}\}_{2n_s \times 1}^T$  and

$$\mathbf{D} = \frac{1}{2} \begin{bmatrix} 1^1 & 0 & 1^1 & 0 & & & & & \\ & 0 & 1^1 & 0 & 1^1 & & & & \\ & & & 1^2 & 0 & 1^2 & 0 & & \\ & & & 0 & 1^2 & 0 & 1^2 & & \\ & & & & & & & \ddots & \\ & & & & & & & & 1^N & 0 & 1^N & 0 \\ & & & & & & & & 0 & 1^N & 0 & 1^N \end{bmatrix}_{2n_s \times 2n_n} \quad (7)$$

is the displacement transformation matrix. Due to the presence of the wall, the incident Rayleigh wave is partially scattered. The total displacement at the wall-soil interface is given by [4]:

$$\mathbf{u}_s = \mathbf{u}_s^i + \mathbf{u}_s^s, \quad (8)$$

in which  $\mathbf{u}_s^i$  and  $\mathbf{u}_s^s$  are the incident and scattered components of the resulting displacement, respectively. The scattered portion can be expressed in terms of the contact tractions  $\mathbf{q}$  through:

$$\mathbf{u}_s^s = \mathbf{U}\mathbf{q}, \quad (9)$$

in which  $\mathbf{U}$  is the influence matrix. The terms within this matrix correspond to the soil influence functions, which are non-singular Green's functions derived by Rajapakse and Wang [1]. For more details about the evaluation of  $\mathbf{U}$ , refer to Carneiro et al. [5]. Substituting eqs. (6) and (9) into eq. (8) yields:

$$\mathbf{D}\mathbf{u}' - \mathbf{U}\mathbf{q} = \mathbf{u}_s^i. \quad (10)$$

Note that the wall is free from external loads, thus  $\mathbf{f} = \mathbf{0}$ . Coupling eqs. (5) and (10), and assembling the terms corresponding to the interface into the full system yields:

$$\left[ \begin{array}{c|c} \bar{\mathbf{K}} & \mathbf{A} \\ \hline \mathbf{D} & \mathbf{0} \end{array} \right] \left[ \begin{array}{c} \mathbf{u} \\ \mathbf{q} \end{array} \right] = \left[ \begin{array}{c} \mathbf{0} \\ \mathbf{u}_s^i \end{array} \right]. \quad (11)$$

### 3.1 Post-processing of contact tractions

The solution of the system in eq. (11) provides the nodal displacements  $\mathbf{u}$  along the wall and the contact tractions  $\mathbf{q}$  at each discretized interface element, from which displacements can be computed anywhere within the half-space. Equation 8 is used to evaluate the displacement fields and quantities deriving from it throughout the soil using the contact tractions.

Strain fields throughout the half-space are obtained using interpolation of displacements between points of a grid. Undeformed and deformed patches of the grid are shown in Fig. 2.

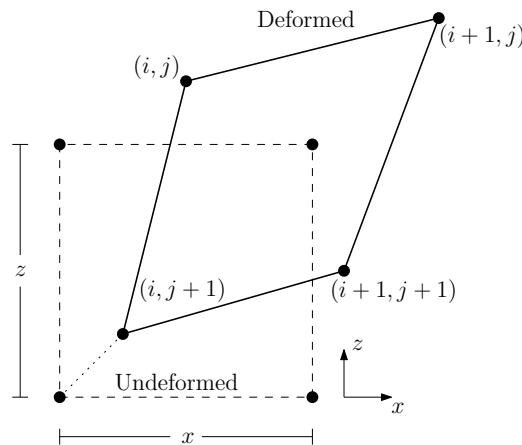


Figure 2. Underfomed and deformed patches of a grid within the half-space.

Assuming that the patches and their deformations are very small, the longitudinal strain fields are calculated through

$$\varepsilon_{ZZ} = \frac{u_z^{(i,j)} - u_z^{(i,j+1)}}{z}, \quad (12)$$

in which  $u_x^{(m,n)}$  and  $u_z^{(m,n)}$  are respectively the horizontal and vertical displacements at node  $m, n$ , and  $z$  is the vertical length of the undeformed patch.

## 4 Numerical results

### 4.1 Validation

Fig. 3 shows normalized horizontal and vertical amplitudes  $U_j^i$  ( $j = x, z$ ) of a rigid footing due to incident Rayleigh waves, in which  $a_0 = \omega(L/2)/c_S$  is the normalized frequency of excitation, in which  $\omega$  is the circular frequency of the Rayleigh wave, and  $c_S = \sqrt{(c_{44}/\rho)}$  is the shear wave speed in the soil. This can be accomplished with the present model by imposing  $h \ll 1$  m, together with making the wall much stiffer than the soil ( $E_w \gg E_s$ ). The isotropic half-space is characterized by Poisson's ratio  $\nu_s = 1/3$ ,  $\rho_s = 1.0 \text{ kg/m}^3$ , and Rayleigh wave velocity  $c_R = 0.9325 c_S$ . The dynamic response of the rigid footing is normalized by the horizontal amplitude of the Rayleigh wave, that is,  $U_j^i = U_j^i/U_x^R$ . The present results are compared with those by Luco and Wong [6] showing good agreement.

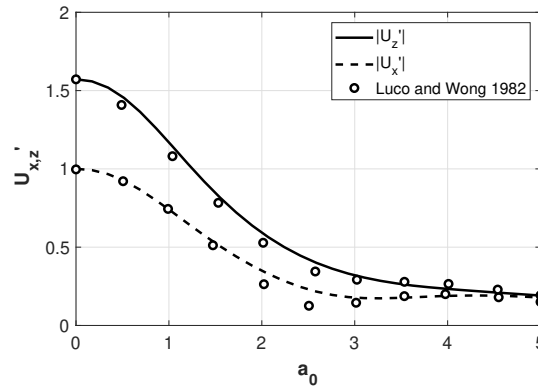


Figure 3. Normalized amplitudes of a rigid footing due to Rayleigh waves.

### 4.2 Ground vibration attenuation

Figure 4 shows the attenuation of horizontal and vertical vibration generated by incident elastic Rayleigh waves impinging on two different types of walls: gabion (G) and soil (S). The wall G has mass density  $\rho = 1700 \text{ kg/m}^3$ , shear wave velocity  $c_S = 300 \text{ m/s}$ , damping factor  $\eta = 0.02$ , and Poisson's ratio  $\nu = 0.2$ , while the wall S is described by  $\rho = 1945 \text{ kg/m}^3$ ,  $c_S = 250 \text{ m/s}$ , pressure wave velocity  $c_P = 1470 \text{ m/s}$ , and  $\eta = 0.025$ . Both walls have  $L = 1 \text{ m}$  and  $h = 3L$ . The representative soil properties used here are the same as material S. The screening efficiency of the wall is measured by the amplitude ratio  $A_r^j = |u_j/u_j^i|$ , where  $u_j$  and  $u_j^i$  are respectively the displacements in the  $j$ -direction with and without the presence of the wall. The results are evaluated at the insertion point ( $x = 0$  and  $z = 0$ ) on a wide frequency range of interest ( $f$  [Hz]). The vertical dashed lines in these graphs mark the natural frequencies of the vibration modes of the corresponding wall under clamped-free boundary conditions. The first flexural vibration mode corresponds to the rocking modes of the wall-soil system. Notice that the flexural natural frequencies are shown in Fig. 4a and the longitudinal natural frequencies are marked in Fig. 4b. The results show that the vibration attenuation maxima are correlated with the respective vibration modes of each wall.

Figure 5 shows the horizontal and vertical amplitude ratio measured behind and far from the wall G, at  $x = 30 \text{ m}$  on the surface of the soil. Carneiro et al. [5] showed that, far from the wall, only attenuated Rayleigh waves remain from the screening effect of the wall. The gray vertical dashed lines mark the frequencies in which the horizontal displacements of the wall are maximum. The first natural frequency corresponds to the rocking vibration mode of the wall. The amplitude ratios are essentially negative, indicating that ground vibrations are attenuated in the entire frequency spectrum. Horizontal and vertical amplitude ratios are approximately equal. Small differences are seen at lower frequencies, in which the body waves travel larger distances due to their larger wavelengths.

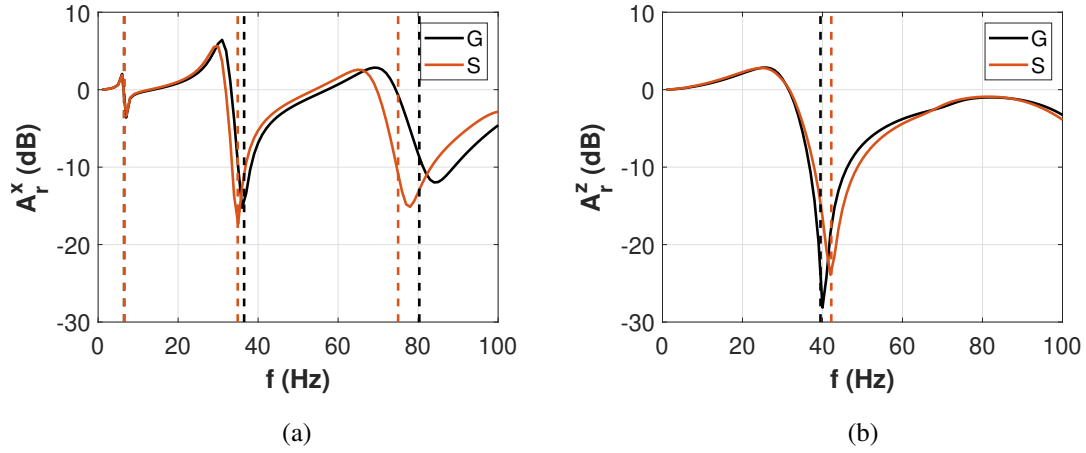
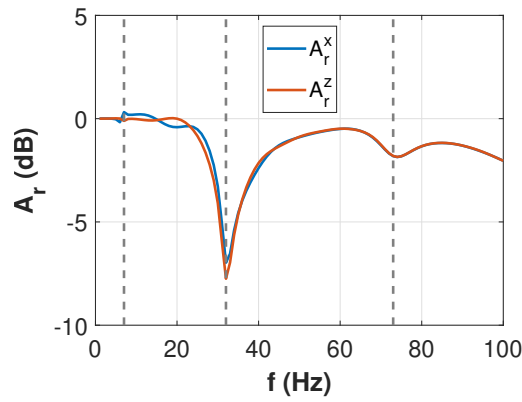


Figure 4. (a) Horizontal and (b) vertical amplitude ratio at the wall-soil interface.


 Figure 5. Horizontal and vertical amplitude ratio at  $x = 30$  m on the surface of the soil.

### 4.3 Wave propagation in the half-space

Figure 6 and 7 shows the free-field motion of Rayleigh waves in the representative elastic soil S ( $\eta_s = 0.01$ ) and the Rayleigh wave-scattering by the wall G with  $L = 1$  m and  $h = 3L$ . These results present displacement and longitudinal strain fields, which are calculated, respectively, using eqs. (8) and (12). The first equation is evaluated through the post-processing of the contact tractions  $\mathbf{q}$  obtained by solving eq. (11). This accurate representation of wave propagation in this unbounded medium is a feature of the boundary element method used in this model.

Figure 6a shows the elastic Rayleigh wave propagation in the positive  $x$ -direction. The excitation frequency is 39.5 Hz, which corresponds to the first longitudinal natural frequency of this wall. Longitudinal strain fields  $\varepsilon_{ZZ}$  are shown, in which red and blue shades corresponding respectively to positive and negative deformations. The amplitudes of strain are larger near the free surface, which is physically consistent for an incident Rayleigh wave. The distance between two consecutive points of the same color corresponds to the Rayleigh wavelength at this frequency.

After the inclusion of the wall (Fig. 6b), Rayleigh wave-scattering phenomena results from the interaction between the Rayleigh wavefront and the wall. Notoriously, the presence of the wall significantly affects the propagation of incident Rayleigh wave, in which part of its energy is converted into body waves. Observe that the scattered waves propagate from the wall to the depth of the soil, without reflecting, which shows the compliance of this model with the Sommerfeld's radiation condition [7].

Figure 7a shows incident Rayleigh wave travelling along the half-space with  $f = 80.3$  Hz, in which this excitation frequency corresponds to the third flexural natural frequency of the wall. A comparison between this result and the lower frequency counterpart (Fig. 6a) clearly indicates that the Rayleigh wavelength is reduced with the increase of the excitation frequency, which is physically consistent. The presence of the wall (Fig. 7b) makes part of the energy from the Rayleigh wave to be converted into body waves. This effect is confined close to the wall, which agrees with the amplitude ratio response in this frequency shown in Fig. 5. The longitudinal strain fields are not significantly changed behind and far from the wall after its installation.

(a) Free-field motion

(b) Rayleigh-wave scattering

Figure 6. Longitudinal strain  $\varepsilon_{ZZ}$  due to Rayleigh waves with  $f = 39.5$  Hz throughout the half-space (a) without and (b) with the wall.

(a) Free-field motion

(b) Rayleigh-wave scattering

Figure 7. Longitudinal strain  $\varepsilon_{ZZ}$  due to Rayleigh waves with  $f = 80.3$  Hz throughout the half-space (a) without and (b) with the wall.

## 5 Conclusions

This article presented the ground vibration attenuation by long surface walls. The Rayleigh-wave scattering was described by strain fields throughout the half-space evaluated through the post-processing from contact tractions of an indirect formulation of the boundary element method. The results show that the strain fields are highly affected due to the presence of body waves scattered by the wall at its surroundings. Behind and far from the wall, the strain fields are not significantly modified with the installation of the wall, which agrees with amplitude ratio results. The present IBEM-FEM model complies with Sommerfeld's Radiation Condition with the scattered waves propagating from the wall to the depth of the soil without reflecting, which shows the physical consistency of the results.

**Authorship statement.** The authors hereby confirm that they are the sole liable persons responsible for the authorship of this work, and that all material that has been herein included as part of the present paper is either the property (and authorship) of the authors, or has the permission of the owners to be included here.

## References

- [1] R. Rajapakse and Y. Wang. Elastodynamic green's functions of orthotropic half plane. *Journal of engineering mechanics*, vol. 117, n. 3, pp. 588–604, 1991.
- [2] V. V. Krylov. Control of traffic-induced ground vibrations by placing heavy masses on the ground surface. *Journal of low frequency noise, vibration and active control*, vol. 26, n. 4, pp. 311–321, 2007.
- [3] A. Dijckmans, P. Coulier, J. Jiang, M. Toward, D. Thompson, G. Degrande, and G. Lombaert. Mitigation of railway induced ground vibration by heavy masses next to the track. *Soil Dynamics and Earthquake Engineering*, vol. 75, 2015.
- [4] G. Fairweather, A. Karageorghis, and P. A. Martin. The method of fundamental solutions for scattering and radiation problems. *Engineering Analysis with Boundary Elements*, vol. 27, n. 7, pp. 759–769, 2003.

- [5] D. Carneiro, P. L. A. Barros, and J. Labaki. Ground vibration attenuation performance of surface walls. *Journal of Sound and Vibration (submitted)*, 2021.
- [6] J. Luco and H. Wong. Response of structures to nonvertically incident seismic waves. *Bulletin of the Seismological Society of America*, vol. 72, n. 1, pp. 275–302, 1982.
- [7] A. Sommerfeld. *Partial differential equations*. Academic Press, 1949.